Coherence and Incoherence in an Optical Comb

Evgeny A. Viktorov,[1,2] Tatiana Habruseva,[3,4,5] Stephen P. Hegarty,[4] Guillaume Huyet,[1,3,4] and Bryan Kelleher[3,4]
[1]National Research University of Information Technologies, Mechanics and Optics, 199034 St. Petersburg, Russia
[2]Optique Nonlinéaire Théorique, Université Libre de Bruxelles, Campus Plaine, Code Postal 231, B-1050 Bruxelles, Belgium
[3]Centre for Advanced Photonics and Process Analysis, and Department of Applied Physics and Instrumentation, Cork Institute of Technology, Cork, Ireland
[4]Tyndall National Institute, University College Cork, Lee Maltings, Dyke Parade, Cork, Ireland
[5]Aston University, Aston Triangle, B4 7ET Birmingham, United Kingdom
(Received 21 January 2013; revised manuscript received 9 October 2013; published 2 June 2014)

We demonstrate a coexistence of coherent and incoherent modes in the optical comb generated by a passively mode-locked quantum dot laser. This is experimentally achieved by means of optical linewidth, radio frequency spectrum, and optical spectrum measurements and confirmed numerically by a delay-differential equation model showing excellent agreement with the experiment. We interpret the state as a chimera state.

DOI: 10.1103/PhysRevLett.112.224101 PACS numbers: 05.45.Xt, 42.60.Fc, 42.65.Sf, 89.75.Kd

Optical frequency combs and in particular, those generated by mode-locked lasers have been at the center of some of the most important research in fundamental physics over the last few decades [1,2]. In a passively mode-locked laser (PML) each line in the comb represents a longitudinal mode of the laser cavity, and each of these modes is specified by three numbers: frequency, phase, and amplitude. That is, each mode in the comb is an oscillator. Unsurprisingly then, many of the theoretical treatments of these lasers exploit the existing language of nonlinear coupled oscillators. Perhaps the most famous theoretical treatment is the master equation formulation of Haus [3], a generalization of the nonlinear Schrödinger equation and the Ginzburg-Landau equation. These equations themselves are used explicitly to describe PMLs in Refs. [4] and [5] among others, and in Ref. [6] the authors showed how to transform the Haus master equation to a Hamiltonian modal formulation. It is sometimes convenient to analyze the electric field of the laser, and the delay-differentiation model of Vladimirov has been shown to be a powerful model for understanding the behavior of PMLs [7]. It was shown in Ref. [8] that it is equivalent to the master equation of Haus, and so it is again formally a coupled oscillator model.

When the oscillator coupling is nonlocal, a surprising phenomenon known as a chimera state can arise. No precise definition exists for such a state, but a typical working definition is a state in which some of the oscillators are mutually coherent but coexist with incoherent drifting oscillators [9,10]. One can deduce that the coupling in a PML must be nonlocal; different modes couple to each other with different coupling strengths, since for a uniform global coupling the optical spectrum would be flat with each mode of equal intensity. This is manifestly not the case.

Despite the intense theoretical activity, experimental realizations of such counterintuitive states in nature have been notoriously difficult to achieve. Thus far, three experimental realizations of chimera states have been reported [11–13]. In each case, the coupling was carefully designed and controlled via computerized feedback. It is desirable to obtain experimental evidence of chimeralike dynamics in a system where the coupling is inherent to the system.

In this Letter, we describe a coexistence of mutually coherent modes and mutually incoherent modes in the comb of a PML. By mutually coherent, we mean the modes are phase locked with fixed relative phase constants between different modes. By mutually incoherent, we mean precisely the opposite: the phase differences between different modes are not fixed and, indeed, are not necessarily even bounded. Each mode has a different frequency, but when all are mutually coherent a periodic pulse train is generated, and conversely, when they are not mutually coherent, irregular dynamics are generated. Experimentally, we investigate the system via several complementary techniques that aim to characterize the mutual coherence and the route to its destabilization. We study the evolution of the radio frequency (rf) spectrum with the pumping current and the corresponding evolution of the optical spectrum. However, one cannot simultaneously measure the phase difference between all modes, and so one needs to tailor the technique to fit the problem. A well-known characteristic of temporal coherence is the modal optical linewidth, and we exploit this easily accessible parameter to analyze our system. Our measurements clearly indicate the loss of coherence in some groups of modes while other modes remain coherent as the pumping current is varied. We perform detailed numerical computations using a system of delay coupled equations and confirm that the coexistence of the coherent and incoherent bunches may have a fundamental origin resulting from nonlinear field-matter interactions. It represents a chimera

state where the coupling is governed inherently by the system itself, requiring neither careful prearrangement nor feedback adaptive algorithms.

In the experiments, the laser used was an uncoated two-section monolithic InAs/GaAs ridge waveguide quantum dot (QD) laser, emitting at 1.3 μm with a repetition rate of 10.2 GHz. The device had an absorber section of 20%, and the temperature was maintained to an accuracy of 10 mK. The absorber bias was −3.0 V for the experiments described here, with a laser threshold of 51 mA at this bias. Figure 1 shows the evolution of the rf spectrum with decreasing forward bias current. The rf spectrum of a PML typically has a peak at the pulse repetition rate of the laser. This frequency is naturally related to the optical spectrum as it equals the modal separation. Working from right to left in Fig. 1, the evolution of the rf and optical spectra is as follows. At 140 mA, there are three groups of modes, and the spectral shape is very reminiscent of bound states observed in Ref. [14]. (We note that in Ref. [15] the development of single-pulse mode locking in microresonators was described, and the optical spectra are suggestive of the appearance of a bound state in the evolution from the multipulse behavior to the single-pulse regime.) As the current is reduced, the optical spectrum evolves as the two redmost groups merge into one large group and the bluemost group gradually shrinks in intensity until it disappears at 100 mA at which point there is only one group of modes formed by the combination of the two redmost groups. Over this region, the rf spectrum changes from a strong central tone surrounded by weak, diffuse tones to a strong central tone again surrounded by weak, diffuse tones but now with the addition of two weak but still prominent sidebands at a current of approximately 120 mA. This general structure holds until 100 mA where the side tones all disappear and only a narrow rf tone remains. At 95 mA, the rf spectrum jumps discretely by approximately 20 MHz, and this is accompanied by a jump in the optical spectrum of approximately 5 nm. From here down to threshold, the rf tone decreases linearly in frequency as previously observed in Ref. [16] while the optical spectrum changes continuously, shrinking in spectral width and intensity until disappearing at threshold. The lower sideband in the region from 100 to 120 mA appears at approximately the continuation of the linearly changing tone found at low currents. Note also that in the regions consisting of the main tone and sidebands, the positions of the sidebands are symmetric but their intensities are not. This is very suggestive of a wave-mixing effect such as that observed in master-slave systems outside of the locking region [17]. From the optical spectrum, it is clear that the sidebands correspond to the birth of a second group of modes. The presence of the sidebands suggests that the two groups are not mutually synchronized. However, the weakness of the tones is strongly suggestive of bounded phase variations [18–20], meaning that the system is synchronized on average. When the current is instead increased, we find that there is a large area of bistability and hysteresis between 95 and 105 mA, and this is also manifest in the optical spectrum, reminiscent of the wavelength bistability observed with QD PMLs in Ref. [21].

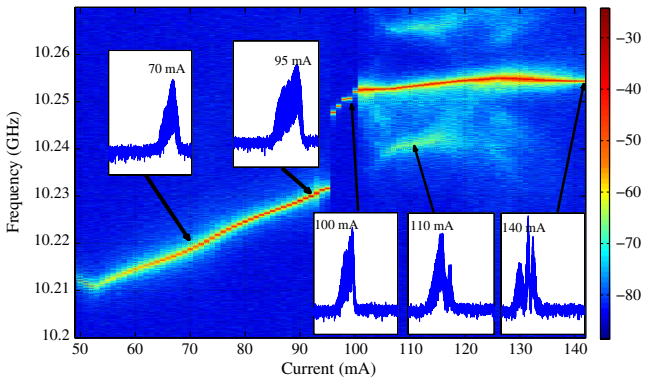

FIG. 1 (color online). Evolution of rf spectrum with current. Color scale in dB. The insets show the optical spectrum (x axis: 225.7 to 230.8 THz) at various points as indicated by the arrows.

As mentioned earlier, to examine the coherence of the modes and different groups we used heterodyne modal linewidth measurements. For a PML where all the modes are mutually coherent, the optical linewidth varies quadratically with the mode number (that is, with the frequency) [3]. Figures 2(a) and 2(b) show zooms of the optical spectrum insets from Fig. 1 and the corresponding linewidth distributions. Figures 2(a) and 2(c) show the optical

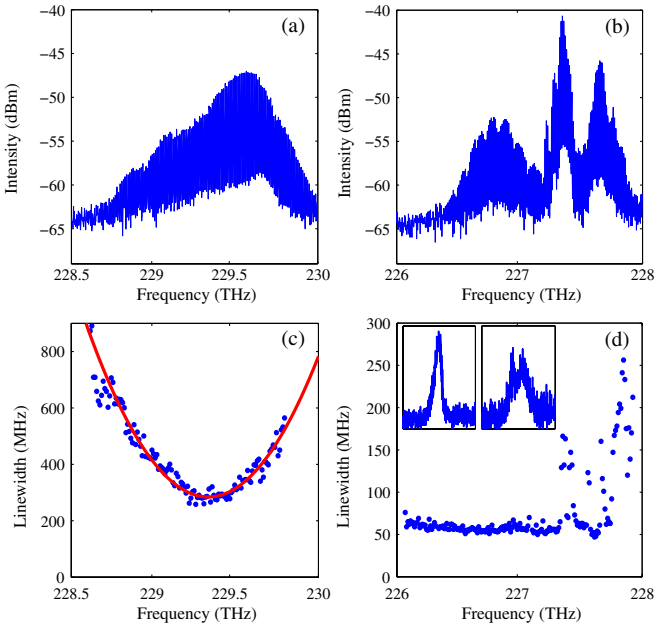

FIG. 2 (color online). (a) Optical spectrum at 70 mA. (b) Optical spectrum at 140 mA. (c) Modal linewidth distribution at 70 mA and best-fit parabola (solid red line). (d) Modal linewidth distribution at 140 mA. The insets show zooms of two individual modes. Left: coherent mode. Right: incoherent mode. The x axis is 400 MHz wide in both cases.

spectrum and the modal linewidth distribution at a current of 70 mA, respectively. The spectrum is asymmetric and consists of one group of modes only. The linewidth distribution is well fitted by a parabola confirming that the output is that of a stable passively mode-locked laser where all the modes are mutually coherent. In Figs. 2(b) and 2(d), the optical spectrum and linewidth distribution at 140 mA are shown. There are three groups of modes. The lowest frequency group is highly coherent with all modes taking almost identical linewidths. The middle group maintains coherence on the red side but develops incoherence in the blue with the modes near the edge of the group taking on relatively high values. The highest frequency group has a large pocket of coherence on the red side near 227.5 THz but for the most part shows a total lack of structure in the linewidth distribution. The insets show zooms of two individual modal line shapes, one from the coherent part of the spectrum and one from the incoherent part of the spectrum. The first is regular and narrow. The second is quite irregular and multipeaked, typical across the incoherent regions. The complete lack of regularity in the distribution suggests incoherence without any phase fixing, and all the modes take on very different values of the linewidth. The spectrum also suggests that the system is not a so-called partially locked system arising from the frequency distribution. In these partially locked cases, the unlocked oscillators are typically those at the edges of the frequency distribution as their frequency differences are too great for the coupling level. In our case, this is manifestly not the situation. Rather, there is a very well-defined group of modes (oscillators) that has lost coherence. This coexistence of coherence and incoherence leads us to conclude that the system is now in a chimera state.

To model the dynamics of our device, we use a set of delay differential equations (DDEs) [7] that has been successfully used to explain various dynamical phenomena observed experimentally [22]. We note that a DDE approach has previously been used in chimera studies [13], although in a very different physical system. Our system reads

$$\gamma^{-1}\partial_t A(t) + A(t) = \sqrt{\kappa} e^{[(1+i\alpha_g)/2]G(t-T)+[(1+i\alpha_q)/2]Q(t-T)} A(t-T), \quad (1)$$

$$\partial_t \rho_{gg} = -\rho_{gg}/\tau + 2F_{gg,ge} - I_g, \quad (2)$$

$$\partial_t \rho_{ge} = -\rho_{ge}/\tau - F_{gg,ge} + W, \quad (3)$$

$$\partial_t \rho_{qg} = -\rho_{qg}/\tau + 2F_{qg,qe} - I_q, \quad (4)$$

$$\partial_t \rho_{qe} = -\rho_{qe}/\tau - F_{qg,qe} - \rho_{qe}/\tau_w, \quad (5)$$

$$\partial_t N = (J-N)/\tau - 4W. \quad (6)$$

$A(t)$ is the normalized complex amplitude of the electric field at the entrance of the absorber section. The delay T is equal to the cold cavity round-trip time. The attenuation factor $\kappa < 1$ describes the total nonresonant linear intensity losses per cavity round trip. The dimensionless bandwidth of the spectral filtering is γ, and the linewidth enhancement factor in the gain (absorber) section is $\alpha_g(\alpha_q)$.

The carrier exchange dynamics for the gain(absorber) section are described by the occupation probabilities $\rho_{gg}(\rho_{qg})$ and $\rho_{ge}(\rho_{qe})$ of the ground state and the first excited state (ES) of a dot, respectively [23]. Escape from the ES to the wetting layer is described by a linear term $\tau_w^{-1}\rho_{qe}$, which strongly depends on the reverse bias. $F_{gg,ge} = \rho_{ge}(1-\rho_{gg})/\tau_g^{\mathrm{cap}} - \rho_{gg}(1-\rho_{ge})/\tau_g^{\mathrm{esc}}$ and $F_{qg,qe} = \rho_{qe}(1-\rho_{qg})/\tau_q^{\mathrm{cap}} - \rho_{qg}(1-\rho_{qe})/\tau_q^{\mathrm{esc}}$ where the parameters $\tau_g^{\mathrm{cap}}(\tau_q^{\mathrm{cap}})$, $\tau_g^{\mathrm{esc}}(\tau_q^{\mathrm{esc}})$ determine the time-dependent recovery of the QD gain(absorber). J is the pump current per dot, and $N(t)$ is the normalized carrier density in the wetting layer of the gain section. $W = N(1-\rho_{ge})/\tau_{ew}^{\mathrm{cap}} - \rho_{ge}/\tau_{ew}^{\mathrm{esc}}$ where $\tau_{ew}^{\mathrm{cap}}(\tau_{ew}^{\mathrm{esc}})$ denote the capture(escape) time for the wetting layer; τ denotes the recombination times in the wetting layer and in the dots, which are taken to be equal for simplicity. The variables $G(t) = g_g[2\rho_{gg}(t)-1]$ and $Q(t) = g_q[2\rho_{qg}(t)-1]$ are the time-dependent dimensionless cumulative saturable gain and absorption, and the parameters $g_{g,q}$ are the differential gains in the corresponding sections. $I_g = s_g e^Q(e^G-1)|A|^2$ and $I_q = s_q(e^Q-1)|A|^2$ [7]. The parameters $s_q > s_g$ are inversely proportional to the saturation intensities of the gain and absorber sections.

In QD lasers, the α factor is quite a delicate parameter and may require more care than with conventional devices [24]. Nonetheless, for many purposes one can assume a constant α, and in the interest of tractability, we do so here. The intensity time trace shown in the inset of Fig. 3(a) displays a typical, regular ML pulse train at $J = 3.2$ (threshold is $J \approx 2.82$). The corresponding optical spectrum is composed of a set of equally spaced modes, all of which are synchronized and highly coherent. The pulse profile becomes asymmetric at $J \approx 3.7$, indicating the formation of a bound state via two groups of modes and a spatial modulation of the phase as described in Ref. [25] leading to the development of trailing edge plateaux (TEP) [25] although the train remains strongly periodic. At $J \approx 3.8$, the spatial modulation develops a temporal component. The plateaux become amplitude modulated, resulting in an overall weak amplitude modulation again suggestive of bounded phase variations. As the current is further increased, the slow envelope develops in a complicated pattern with multiple harmonics (affecting only the plateaux), all in excellent qualitative agreement with the experimental rf diagram.

Further increase of the current leads to multiple transformations of the optical comb in which coherent and incoherent modal bunches may coexist. Several intensity pulses at $J = 5.5$ are shown in the inset of Fig. 3(b). The peak intensity remains almost unchanged from pulse to

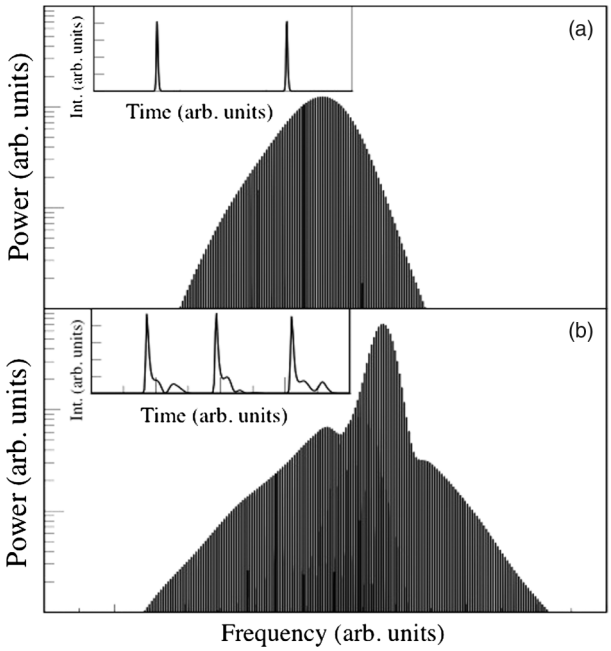

FIG. 3. (a) Optical spectrum at $J = 3.2$. The inset shows two regular pulses from the associated periodic pulse train. (b) Complicated optical spectrum at $J = 5.5$. The inset shows three nonconsecutive pulses from the associated irregular pulse train. The other parameters are $\tau_g^{\mathrm{cap}} = \tau_q^{\mathrm{cap}} = 2$ ps; $\tau_g^{\mathrm{esc}} = 20$ ps; $\tau_q^{\mathrm{esc}} = \tau_w = 10$ ps; $\tau = 0.5$ ns; $\tau_{ew}^{\mathrm{cap}} = 5$ ps; $\tau_{ew}^{\mathrm{esc}} = 50$ ps; $\gamma = 10$; $T = 150$ ps; $\kappa = 0.35$; $s_q/s_g = 30$; $\alpha_g = \alpha_q = 2$; $g_g = 8.5$; $g_q = 1.5$.

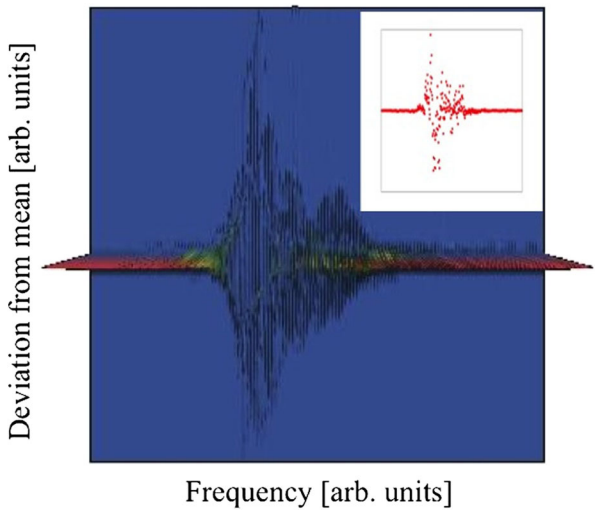

FIG. 4 (color online). Plot of the jitter analysis of the filtered time series. The x axis measures the position of the filter, and the y axis measures the coherence. Time is normalized to 5 ps, and the parameters are the same as in Fig. 3(b). The inset shows a snapshot of the deviations.

pulse while the trailing edge varies significantly. (Note that the pulses shown are nonconsecutive.) Typically, chimera states are bistable with either a fully synchronous or a fully asynchronous state, and in this work the chimera is bistable with a fully synchronous harmonic mode-locked state [26].

We filter the electric field $A(t)$ of Eqs. (1)–(6) and analyze the modal behavior via a jitter analysis of the filtered time series. (The timing jitter of a PML is directly related to the modal linewidths as shown in Ref. [27], for example.) Again, we exploit the physics of the system to analyze the phase relationships. A periodic pulse train in a semiconductor laser is formed by the simultaneous lasing of a number of longitudinal modes with fixed relative phase constants. We examine the intensities corresponding to small groups of modes, and where the resulting intensity is a regular train we can deduce that the modes have fixed relative phases: coherence. For groups where the intensity fluctuates irregularly, we can deduce that they do not have fixed relative phases: incoherence. It is only in the behavior of *groups* of modes that this is revealed.

Each vertical line in Fig. 4 is a distribution measuring the coherence of five successive modes of the spectrum. Narrow distributions correspond to *statistically* strong coherence and broad distributions to incoherence. The distributions at the wings of the optical spectrum are very narrow, and so here the modes are coherent. In stark contrast, most of the central groups of the spectrum have very broad distributions and, thus, are incoherent. Note the pockets of coherence even within the primarily incoherent part similar to the experimental case, reminiscent of many-headed chimera behavior [13,28,29]. The inset shows a snapshot of the analysis.The similarity with the phase snapshots of Ref. [10] is clear.

The path to the chimera both numerically and experimentally begins with strong synchronization throughout the system. As the current is increased, the modes break into several groups and a spatial structure develops with a possible bounded phase modulation corresponding to synchronization on average. Finally, one group (or more) of modes loses synchronization, resulting in the formation of the chimera. This is precisely the path described in Ref. [10].

Two aspects central to the appearance of the chimera are the material type and the device length. The presence of the TEP in QD devices is the first step towards the chimera. One can physically reason that it is the Pauli blocking inherent to the dots that promotes the TEP. As the current is increased, the dot occupation probability gets closer to 1. In PML devices, there is typically a fast and slow stage in the recovery of the gain, and as the dots are filled the slow stage dominates, becoming increasingly sensitive to perturbations and eventually unstable. There is no equivalent saturation in quantum-well-based devices. The only other variable parameter is the device length. The effect of decreasing the length can be ascertained from previous works on QD PML devices. Experimental studies of rf spectra were obtained in Ref. [16] on a much shorter QD device (repetition rate of about 16 GHz as against 10 GHz

here). There was no evidence of chimeralike properties in Ref. [16]. The bound state and TEP phenomenon was found numerically in Ref. [25], again for a much shorter device. Nonetheless, no evidence of a chimera state was obtained. The importance of the length can be ascribed to the consequent lower modal separation and, hence, greater intermodal interactions.

In conclusion, we demonstrate a coexistence of coherent and incoherent modes in an optical comb that we interpret as a chimera state. DDE modeling is in excellent qualitative agreement with experimental observations.

The authors gratefully acknowledge David Goulding for very useful discussions and assistance in manuscript preparation. This work was conducted under the framework of the INSPIRE programme funded by the Irish Government's Programme for Research in Third Level Institutions Cycle 5, National Development Plan 2007-2013 with the assistance of the European Regional Development Fund. The authors also gratefully acknowledge the support of Science Foundation Ireland under Contract No. 11/PI/1152.

[1] S. A. Diddams, D. J. Jones, J. Ye, S. T. Cundiff, J. L. Hall, J. K. Ranka, R. S. Windeler, R. Holzwarth, T. Udem, and T. W. Hänsch, Phys. Rev. Lett. **84**, 5102 (2000); J. Reichert, M. Niering, R. Holzwarth, M. Weitz, Th. Udem, and T. W. Hänsch, Phys. Rev. Lett. **84**, 3232 (2000); Th. Udem, R. Holzwarth, and T. W. Hänsch, Nature (London) **416**, 233 (2002).

[2] D. J. Jones, S. A. Diddams, J. K. Ranka, A. Stentz, R. S. Windeler, J. L. Hall, and S. T. Cundiff, Science **288**, 635 (2000).

[3] H. A. Haus, IEEE J. Sel. Top. Quantum Electron. **6**, 1173 (2000); Y. Takushima, H. Sotobayashi, M. Grein, E. Ippen, and H. Haus, Proc. SPIE Int. Soc. Opt. Eng. **5595**, 213 (2004).

[4] Q. Quraishi, S. T. Cundiff, B. Ilan, and M. J. Ablowitz, Phys. Rev. Lett. **94**, 243904 (2005).

[5] N. N. Akhmediev, J. M. Soto-Crespo, and G. Town, Phys. Rev. E **63**, 056602 (2001).

[6] A. Gordon and B. Fischer, Phys. Rev. Lett. **89**, 103901 (2002).

[7] A. G. Vladimirov and D. Turaev, Phys. Rev. A **72**, 033808 (2005).

[8] T. Kolokolnikov, M. Nizette, T. Erneux, N. Joly, and S. Bielawski, Physica (Amsterdam) **219D**, 13 (2006).

[9] Y. Kuramoto and D. Battogtokh, Nonlinear Phenom. Complex Syst. **5**, 380 (2002).

[10] D. M. Abrams and S. H. Strogatz, Phys. Rev. Lett. **93**, 174102 (2004); D. M. Abrams, R. Mirollo, S. H. Strogatz, and D. A. Wiley, Phys. Rev. Lett. **101**, 084103 (2008); E. A. Martens, C. R. Laing, and S. H. Strogatz, Phys. Rev. Lett. **104**, 044101 (2010); D. M. Abrams and S. H. Strogatz, Int. J. Bifurcation Chaos Appl. Sci. Eng. **16**, 21 (2006).

[11] A. M. Hagerstrom, T. E. Murphy, R. Roy, P. Hövel, I. Omelchenko, and E. Schöll, Nat. Phys. **8**, 658 (2012).

[12] M. R. Tinsley, S. Nkomo, and K. Showalter, Nat. Phys. **8**, 662 (2012).

[13] L. Larger, B. Penkovsky, and Y. Maistrenko, Phys. Rev. Lett. **111**, 054103 (2013).

[14] M. Butkus, E. A. Viktorov, T. Erneux, C. J. Hamilton, G. Maker, G. P. A. Malcolm, and E. U. Rafailov, Opt. Express **21**, 25526 (2013).

[15] M. R. E. Lamont, Y. Okawachi, and A. L. Gaeta, Opt. Lett. **38**, 3478 (2013).

[16] F. Kéfélian, S. O'Donoghue, M. T. Todaro, J. McInerney, and G. Huyet, Opt. Express **17**, 6258 (2009).

[17] J. M. Liu and T. B. Simpson, IEEE J. Quantum Electron. **30**, 957 (1994).

[18] P. A. Braza and T. Erneux, Phys. Rev. A **41**, 6470 (1990).

[19] B. Kelleher, D. Goulding, B. Baselga Pascual, S. P. Hegarty, and G. Huyet, Phys. Rev. E **85**, 046212 (2012).

[20] J. Thévenin, M. Romanelli, M. Vallet, M. Brunel, and T. Erneux, Phys. Rev. Lett. **107**, 104101 (2011).

[21] K. Silverman, M. Feng, R. Mirin, and S. Cundiff, in *Quantum Dot Devices*, edited by Z. M. Wang (Springer, New York, 2012), Chap. 2, p. 23.

[22] M. Radziunas, A. G. Vladimirov, E. A. Viktorov, G. Fiol, H. Schmeckebier, and D. Bimberg, IEEE J. Quantum Electron. **47**, 935 (2011).

[23] T. Piwonski, J. Pulka, G. Madden, G. Huyet, J. Houlihan, E. A. Viktorov, T. Erneux, and P. Mandel, Appl. Phys. Lett. **94**, 123504 (2009).

[24] B. Lingnau, K. Lüdge, W. W. Chow, and E. Schöll, Phys. Rev. E **86**, 065201 (2012).

[25] M. Radziunas, A. G. Vladimirov, E. A. Viktorov, G. Fiol, H. Schmeckebier, and D. Bimberg, Appl. Phys. Lett. **98**, 031104 (2011).

[26] E. A. Viktorov, P. Mandel, M. Kuntz, G. Fiol, D. Bimberg, A. G. Vladimirov, and M. Wolfrum, Appl. Phys. Lett. **91**, 231116 (2007).

[27] R. Rosales, K. Merghem, A. Martinez, F. Lelarge, A. Accard, and A. Ramdane, Opt. Express **20**, 9151 (2012).

[28] I. Omelchenko, O. E. Omel'chenko, P. Hövel, and E. Schöll, Phys. Rev. Lett. **110**, 224101 (2013).

[29] S. R. Ujjwal and R. Ramaswamy, Phys. Rev. E **88**, 032902 (2013).